

# Global Spread, Genetic Differentiation, and Selection of Barley Spot Form Net Blotch Isolates

Kealan Hassett,<sup>1</sup>  Mariano Jordi Muria-Gonzalez,<sup>1</sup>  Anke Martin,<sup>2</sup>  Aziz Karakaya,<sup>3</sup> Arzu Çelik Oğuz,<sup>3</sup> József Bakonyi,<sup>4</sup> Noel L. Knight,<sup>1,2</sup> Renée Prins,<sup>5</sup> and Simon R. Ellwood<sup>1,†</sup> 

<sup>1</sup> Centre for Crop and Disease Management, School of Molecular and Life Sciences, Curtin University, Bentley, WA 6102, Australia

<sup>2</sup> Centre for Crop Health, University of Southern Queensland, Toowoomba, QLD 4350, Australia

<sup>3</sup> Department of Plant Protection, Faculty of Agriculture, Ankara University, Dışkapı, Ankara 06110, Turkey

<sup>4</sup> Plant Protection Institute, HUN-REN Centre for Agricultural Research, Herman Ottó str. 15, 1022 Budapest, Hungary

<sup>5</sup> CenGen (Pty) Ltd., Worcester, 6850, South Africa

Accepted for publication 14 April 2024.

## Abstract

Spot form net blotch, caused by *Pyrenophora teres* f. *maculata*, is a significant necrotrophic disease of barley that spread worldwide in the twentieth century. Genetic relationships were analyzed to determine the diversity, survival, and dispersal of a diverse collection of 346 isolates from Australia, Southern Africa, North America, Asia Minor, and Europe. The results, based on genome-wide DArTseq data, indicated that isolates from Turkey were the most differentiated with regional sub-structuring, together with individuals closely related to geographically distant genotypes. Elsewhere, population subdivision related to country of origin was evident, although low levels of admixturing was found that may represent rare genotypes or migration from unsampled populations.

Canadian isolates were the next most diverged, and Australian and South African the most closely related. With the exception of Turkish isolates, multiple independent *Cyp51A* mutation events (which confer insensitivity to demethylation inhibitor fungicides) between countries and within regions was evident, with strong selection for a transposable element insertion at the 3' end of the promoter and counterselection elsewhere. Individuals from Western Australia shared genomic regions and *Cyp51A* haplotypes with South African isolates, suggesting a recent common origin.

**Keywords:** diversity arrays technology, fungicide resistance, *Hordeum vulgare*, soft selective sweeps

Spot form net blotch is a major disease of barley, causing yield losses of up to 20% in susceptible cultivars in Australia and quality downgrades associated with increased levels of undersized grain (McLean et al. 2022). The disease is caused by *Pyrenophora teres* f. *maculata* (*Ptm*), a filamentous ascomycete within the class Dothideomycetes. *Ptm* is closely related to, but genetically distinct from, *P. teres* f. *teres* (*Ptt*; Ellwood et al. 2012; Syme et al. 2018), the cause of net form net blotch, producing ovoid rather than net-like striated disease symptoms. *Ptm* is classed as a hemi-biotroph, with a short asymptomatic or biotrophic phase followed by necrotrophy (Liu et al. 2011). Although hybridization may occur between the two pathogens, this is uncommon (Poudel et al. 2017, 2019) with hybrids showing lower fitness in planta, reduced recombination rates and negative epistasis between parental alleles at several loci (Yuzon et al. 2023). Different genetic interactions with barley, governed by numerous major and minor host genes (Clare et al. 2020), supports their genetic autonomy.

The first definitive report of spot form net blotch was by Smedegård-Petersen (1971) in Denmark, and the disease has since emerged as a notable disease on commercial barley across all major growing regions (reviewed in McLean et al. 2009). The pathogen persists in stubble as pseudothecia containing ascospores, with both

ascospores and later asexual conidia from diseased plants dispersed by air turbulence and water splash (Liu et al. 2011). This dual mode of propagation allows for both recombination and clonal expansion, rapidly disseminating new alleles, gene combinations, or fungicide resistance mutations that provide an adaptive advantage (Mair et al. 2020; Muria-Gonzalez et al. 2023). Hemi-biotrophs and necrotrophs secrete effectors that noticeably induce cell death (Faris and Friesen 2020). Susceptibility is dominant in the host, with recessive resistance resulting from the loss or mutation of genes encoding proteins targeted by pathogen effectors (Muria-Gonzalez et al. 2023; Peters Haugrud et al. 2019). This is known as the inverse gene-for-gene model, in contrast to dominant host resistance against biotrophs that selects for advantageous alleles or mutations in the pathogen population, such as the loss or alteration of the corresponding pathogen effector gene (Ellwood et al. 2024; Lu et al. 2016). Notable exceptions to the conventional gene-for-gene model are the recessive *mlo* and *rbgh2* genes that prime host defenses against powdery mildews (Ge et al. 2016, 2020; Moolhuijzen et al. 2023). Both models occur in net blotch–barley interactions (Liu et al. 2011; Muria-Gonzalez et al. 2023; Williams et al. 1999), with early host detection of the pathogen at the asymptomatic or biotrophic phase likely determining gene-for-gene resistance, followed by the inverse model in the necrotrophic phase.


The strategic development of durable host resistance and integration with other disease control methods requires an understanding of a pathogen's genetic diversity and population structure, as well as the evolutionary potential and overall population dynamics (McDonald and Linde 2002). These are dependent on understanding a range of different processes including genetic drift, gene flow, selection, population bottlenecks, and the contributions of the sexual and asexual stages to maintaining populations. For example, the challenge presented by *Ptt* was illustrated in an international study by Dahanayaka et al. (2021b), which suggested high levels of

†Corresponding author: S. R. Ellwood; srellwood@gmail.com

**Funding:** Support was provided by the Grains Research and Development Corporation (CUR2001-002RSX).

**e-Xtra:** Supplementary material is available online.

The author(s) declare no conflict of interest.

 Copyright © 2024 The Author(s). This is an open access article distributed under the CC BY 4.0 International license.

migration between countries, but also regional clustering. An Australian study by Linde and Smith (2019) reflected these results, demonstrating a panmictic population structure across the country, likely maintained by extensive gene flow between regions, but also evidence for elevated linkage disequilibrium levels, which the authors ascribed to the restricted host diversity of barley monocultures, together with host genotype adaptation. Genetic diversity studies of *Ptm* have been made in several countries: Algeria (Ahmed Lhadj et al. 2022), Australia (Bogacki et al. 2010; Hassett et al. 2023; Lehmsiek et al. 2010; McLean et al. 2014; Serenius et al. 2007), Canada (Akhavan et al. 2016), Iran (Vasighzadeh et al. 2021), the Republic of South Africa (RSA; Campbell et al. 2002; Lehmsiek et al. 2010), Sardinia (Rau et al. 2003), and Turkey (Çelik Oğuz et al. 2019). These studies found high levels of genetic diversity and low levels of clonality and, with the exceptions of Iran (Vasighzadeh et al. 2021) and in a comparison between Australia and the RSA (Lehmsiek et al. 2010), little evidence for regional genetic differentiation.

The *Ptm* studies above used a variety of genetic marker methods including random amplified polymorphic DNA, amplified fragment length polymorphisms, and simple sequence repeats (SSRs). Random amplified polymorphic DNA and amplified fragment length polymorphisms use anonymous markers, meaning they lack genomic context and often have distorted genomic distribution. SSRs are hypervariable, limiting phylogenetic inferences but enabling individuals to be resolved, and typically low numbers are used, which also limits genomic representation. DArTseq is a highly parallel genome-wide approach pioneered by Jaccoud et al. (2001), in combination with next-generation sequencing (Sansaloni et al. 2011), and is based on a restriction enzyme complexity reduction step, which selects for low-copy and gene-rich coding DNA. The DArT system produces both dominant SilicoDArT markers and co-dominant DArTseq single-nucleotide polymorphism (SNP) markers. Such dense marker sets allow finer resolution of population structure in fewer samples compared with hypervariable SSRs (Jeffries et al. 2016) and greater resolution of admixturing and hybridization events than previous methods (Melville et al. 2017). In Western Australia, where the most popular recent barley varieties are susceptible to spot form net blotch (Shackley et al. 2021), DArTseq enabled Hassett et al. (2023) to infer genotypic clustering unrelated to geographic origin but associated with the C14 $\alpha$ -demethylase (*Cyp51A*) gene, mutations of which confer resistance to demethylation inhibitor (DMI, or triazole) fungicides (Mair et al. 2020).

Analyses of *Ptm* populations so far have been limited to isolates representing relatively small geographical regions, whereas a comparative study of geographically diverse populations would provide a valuable perspective on regional relationships. In this study, we compared the intercontinental population structure and genetic diversity of *Ptm* isolates from Australia, Canada, Denmark, Hungary, the RSA, and Turkey. The main objectives were to investigate the genetic relationships between isolates from different countries and their potential for global spread. This was based on Bayesian and multivariate clustering methodologies, which are effective in detecting admixture or migration events, together with evolutionary relationships based on genetic distance, molecular variance, and population differentiation measures. In Australia, high levels of DMI resistance have recently developed in *Ptm* (Mair et al. 2020). We therefore compared the *Cyp51A* haplotypes and their resistance phenotypes in the collection to determine if resistance arose as independent events.

## Materials and Methods

### Fungal material

The metadata for 346 *Ptm* isolates used in this study are provided in Supplementary Table S1a. Live cultures consisted of the following: 24 Turkish isolates collected from 16 locations between 2012

and 2015 (Çelik Oğuz et al. 2019); 16 RSA isolates collected in 2016 from five locations in the Western Cape; and 283 isolates collected from four regions in Australia, with the majority from Western Australia ( $n = 224$ ), followed by Victoria (Vic;  $n = 31$ ), South Australia (SA;  $n = 20$ ) and a region straddling the border of Queensland and New South Wales (Qld and NSW;  $n = 8$ ). Preexisting DArT data for 251 Australian isolates, collected between 2016 and 2020, were published by Hassett et al. (2023). These samples are highlighted in Supplementary Table S1a. Additional live isolates included in this study were a DMI sensitive control isolate, U7, collected in 2012 (Mair et al. 2020); isolate M3, collected in 2009, which possesses virulence against a seedling resistance gene (Muria-Gonzalez et al. 2023); and isolate M4 sampled from the same site. The *Ptm* reference genome assembly isolate SG1 (Syme et al. 2018), collected in 1996, was used as a standard control between DArTseq genotyping runs.

DNA was provided for 10 Hungarian isolates originating from four locations. Most were collected from 2017 to 2018, one from 2007 (H-160), and one from 1992 (H-117.1/1). Twenty-four RSA isolates, collected in 2007 from three locations in the Western Cape (Lehmsiek et al. 2010), together with H-1016 from Hungary, were used for PCR amplification and sequencing of the *Cyp51A* gene and promoter only as the DNA quality was not suitable for DArTseq (Supplementary Table S1b). *Cyp51A* data for isolates 17FRG089 and 18FRG195 were obtained from Mair et al. (2020), representing promoter haplotypes H3 and H5.

Preexisting DArTseq genotype data from USQ was included for 12 isolates from Canada, collected by Akhavan et al. (2015, 2016) between 2010 and 2011 from the provinces of Alberta, Manitoba, and Saskatchewan. DArTseq data were also provided for the 16 RSA *Ptm* isolates described above, and the two older Hungarian isolates (H-160 and H-117.1/1), Western Australian isolate U7 (Dahanayaka et al. 2021a), and a type culture from Denmark, CBS 228.76, collected by V. Smedegaard-Petersen at an unknown date, but presumed to be from the 1970s.

### Fungal isolation, DNA extraction, and genotyping

Single-spored cultures of Western Australian *Ptm* samples collected in 2021 were made by surface sterilizing diseased leaf samples before storage as mycelia agar plugs at  $-80^{\circ}\text{C}$  (Hassett et al. 2023). Genomic DNA was extracted from 7-day-old V8-PDA cultures (150 ml/liter of V8 juice [Campbell's Soups Australia, Lemnos, VIC, Australia], 10 g/liter of Difco potato dextrose agar [Becton Dickinson, Sparks, MD], 10 g/liter of agar [Sigma Aldrich, St. Louis, MO], and 3 g/liter of  $\text{CaCO}_3$ ) by scraping mycelia from a single plate. The tissue was freeze-dried in 1.5-ml tubes, and DNA was extracted using a Wizard Genomic DNA Purification Kit (Promega, Fitchburg, WI) in accordance with the manufacturer's protocol. DNA concentration and quality were measured with a NanoDrop spectrophotometer (Thermo Fisher Scientific, Waltham, MA). DNA used for sequencing the *Cyp51A* gene and promoter of isolates from Australia, the RSA, and Turkey was extracted by the same method. DNA provided by collaborators for the Hungarian and RSA 2007 isolates was extracted by the cetyl trimethyl ammonium bromide method described by Saghai Maroof et al. (1994). DArTseq genotyping was performed as described in Hassett et al. (2023) by Diversity Arrays Technology Pty Ltd. (Canberra, Australia). Genome complexity reduction was achieved with *Pst*I and *Mse*I restriction enzymes, followed by ligation with adapters compatible with the restriction enzyme cleavage sites and containing a sample barcode region before next-generation sequencing on a HiSeq2000 DNA platform (Illumina, San Diego, CA). Illumina sequences were processed using proprietary DArT analytical pipelines (Sánchez-Sevilla et al. 2015). In a primary pipeline, FASTQ files are filtered for poor-quality sequences, applying stringent selection criteria to the barcode region of adapters to assign sequences to specific samples. Identical sequences are collapsed into FASTQCOL files, which are then used in a secondary

pipeline to call SNP and silicoDARt polymorphisms. The genomic locations of DNA fragments were obtained by BLASTN against a local database containing the *Ptm* isolate SG1 reference genome assembly (GenBank GCA\_900231935), with an expected value (E) of  $<5e^{-7}$  and a minimum nucleotide identity of 70%.

### Integrating DARt data from different genotyping assays and data filtering

Data from different DARtseq genotyping runs were merged in Excel based on AlleleID, which refers to specific genetic markers (both SNP and SilicoDARt) and their alleles. Only markers in common between three independent DARt runs were retained. Data were filtered using *poppr* v 2.8.3 (Kamvar et al. 2014) within RStudio 4.2.0 (RStudio, Boston, MA) to remove markers and isolates with greater than 10% missing data using the *missingno* command. Phylogenetically uninformative loci, those containing less than a given percentage of divergent individuals (cutoff =  $2/n$ , where  $n$  is the number of individuals in a given population) and a minimum allele frequency of less than 0.01, were also removed using the *informloci* command. The resultant SNP and silicoDARt data are provided in Supplementary Table S2a and b, respectively, and at <https://doi.org/10.25917/9ezd-6v72>.

### Identification of multilocus genotypes

To account for genotyping errors that may result in isolates being placed in different multilocus genotypes (MLGs), the minimum genetic distance between *Ptm* isolate SG1 replicates in each DARt plate was established. At least one SG1 replicate per plate within each DARtseq run was used and a distance matrix calculated in *poppr* v 2.8.3 (Kamvar et al. 2014) using the *prevosti.dist* function. The maximum genetic distance between SG1 replicates provided the minimum cutoff score to classify independent MLGs using the *mlg.filter* command. Clones within the same MLG were removed from subsequent analyses using the *poppr.clonecorrect* function.

### Genetic diversity, linkage disequilibrium, and analysis of molecular variance

Genetic diversity indices for groups of isolates were generated within *poppr* v 2.8.3 (Kamvar et al. 2014) using the *poppr* function. Indices were determined by comparing the number of MLGs to the expected number of MLGs in the original data and calculating Simpson's corrected index ( $(N/(N - 1))\lambda$ ) of MLG diversity, Nei's unbiased gene diversity index, and the Shannon–Wiener index of MLG group genotypic diversity. The extent of random mating occurring within populations was determined by calculating gametic equilibrium using the standardized index of association ( $\bar{r}_d$ ), which is independent of sample size (Agapow and Burt 2001), using 999 permutations. Analysis of molecular variance differentiation statistics of groups, based on their regional collection sites, were calculated by using *poppr.amova*. Significance was measured using the *randtest* command with 10,000 repetitions. Pairwise PhiPT, to measure population differentiation, was calculated for clone-corrected groups within GenAlEx 6.5 with 999 permutations (Peakall and Smouse 2006, 2012).

### Phylogenetic tree construction

Genetic relationships among clone-corrected isolates were examined using genetic distance data based on the Prevosti's absolute genetic distance (Prevosti et al. 1975) and calculated using the *prevosti.dist* command in *poppr* v 2.8.3 (Kamvar et al. 2014). Gene sequence SNPs were coded as a single-nucleotide variation, and *Cyp51A* promoter transposon insertion variants were coded as presence or absence (1 = transposon variant present, 0 = absent) within Genalex (Peakall and Smouse 2012). Branch support values were calculated with 1,000 bootstrap replicates in *poppr* v 2.8.3 using the *aboot* command. To simplify the dendrogram in Figure 1, Australian isolates were reduced in number by random sampling of isolates from the main Australia collection but retaining the *Ptm*

genome reference isolate SG1 and isolates with a highly resistant (HR) fungicide phenotype, as STRUCTURE and DAPC results suggested admixturing. Figure 1 branch tips were linked to geolocations via the *phylo.to.map* command in *phytools* v 1.9.16 (Revell 2012).

### Genetic clustering and subdivision analyses

Genetic relationships on the entire clone-corrected collection of isolates were compared by principal component analysis (PCA), discriminant analysis of principal components (DAPC), and Bayesian inference in the program STRUCTURE v 2.3.4 (Pritchard et al. 2000). PCA and DAPC do not make a priori assumptions of population structure, with DAPC optimized for large datasets and providing a higher resolution than PCA of between-group variability and population structures among clusters (Jombart et al. 2010). STRUCTURE is a model-based clustering approach that assumes Hardy–Weinberg equilibrium among loci and is able to accommodate admixture linkage disequilibrium to detect population subdivisions (Falush et al. 2003).

PCA was performed using the *glpca* function in the R package *adegenet* to observe the impact of eigenvalues on the overall variance explained (Jombart 2008). DAPC was performed using the *find.clusters* command in *adegenet* to produce a *K*-means clustering graph with the lowest Bayesian information criteria, then using the appropriate value for each of the DAPC analyses. DAPC analyses were then run using the *dapc* command, based on the cross-validation function *Xval.dapc* result to retain the correct number of principal components (Dray and Dufour 2007). STRUCTURE was run with a burn-in period of 100,000 steps and 100,000 replications, assessing *K* values between one and nine, with 10 iterations. The STRUCTURE output data were parsed through STRUCTURE HARVESTER (Earl and von Holdt 2012) to determine the optimal *K* value.

### *Cyp51A* promoter and gene DNA sequencing

The *Cyp51A* coding region and 846 bp of the promoter were amplified and direct Sanger sequenced as described in Mair et al. (2016). However, two new reverse primers were made to improve sequence quality close the 3' end of *Cyp51A* due to the proximity of mutations. These were (5'-3'): PtCyp51A\_4F GGTATCTCAGC CAACAGCG, nested within the gene, and PtCyp51A\_4R GCACTCGTGGTACGTACTGC, which is located after the stop codon. DNA concentrations were measured with a NanoDrop spectrophotometer (Thermo Fisher Scientific) and single amplicons verified by electrophoresis in a 1% agarose gel. PCR products were sequenced by Macrogen (Seoul, South Korea) on an Applied Biosystems ABI3730xl DNA Analyzer 96-capillary array (Thermo Fisher Scientific). *Cyp51A* gene and promoter sequences were aligned against the *Ptm* reference isolate SG1 (assembly GCA\_900231935, GenBank accession MT499776 and surrounding regions) in Geneious 8.0.1 (Biomatters, Auckland, New Zealand) using the MUSCLE alignment tool, then visually inspected for polymorphisms. DNA sequences are available from GenBank under accessions OR734722 to OR734732, OR751399, OR751400, OR734239 to OR734251, and OP753350 to OP753352.

### In vitro fungicide sensitivity phenotypes

*Ptm* isolates were tested against six concentrations of tebuconazole: 0, 2.5, 5, 7.5, 10, and 20  $\mu\text{g ml}^{-1}$ . Canadian, Hungarian, and RSA 2007 isolates were not included, as no live cultures were available. Isolates were grown for 5 days on a V8-PDA plate, then approximately 50 mg of hyphae was scraped from the surface and homogenized in a 1.5-ml Eppendorf tube before adding 200  $\mu\text{l}$  of sterilized deionized water. Ten microliters of inoculum was transferred into 75  $\mu\text{l}$  of yeast Bacto acetate media (10 g of yeast extract, 10 g of Bacto peptone, and 10 g of sodium acetate per liter, amended to one of the six tebuconazole concentrations above) in 96-well plates (Corning, NY), with three biological replicates per isolate. Isolate growth was visually assessed at 3 and 5 days postinoculation,

based on the presence or absence of mycelia with the latter verified under a binocular microscope. Isolates showing no hyphal growth were considered sensitive at a given concentration. Those where hyphal growth was evident between 2.5 and 5  $\mu\text{g ml}^{-1}$  were scored as moderately resistant (MR, none of these isolates grew at 7.5  $\mu\text{g ml}^{-1}$ ), and isolates with hyphal growth at 10  $\mu\text{g ml}^{-1}$  were scored as highly resistant (HR). No isolates grew at 20  $\mu\text{g ml}^{-1}$ .

#### Minimum spanning networks based on *Cyp51A* haplotype data

The Excel add-in GenAIEx v 6.5 (Peakall and Smouse 2006, 2012) was used to manually curate the location and nucleotide identity of each SNP in the *Cyp51A* gene and promoter region. The data were imported into *poppr* v 2.8.3 (Kamvar et al. 2014) within RStudio 4.2.0 using the *getfile* command. Provesti's genetic distance (Prevosti et al. 1975) was used to produce minimum spanning networks using the *provesti.distance* function. Haplotype networks were constructed using the *plot\_poppr\_msn* command. Within each node, isolates were grouped to represent the country of origin and fungicide resistance phenotype, whereas node sizes and their sectors were scaled to indicate the number of isolates from a given group.

## Results

### Detection of MLGs

DArTseq genotyping of *Ptm* samples provided a total of 2,193 SNPs and 5,092 SilicoDArT markers shared between independent

DArTseq runs (Supplementary Table S2a and b). Of these, 543 SNPs and 690 SilicoDArT markers were retained for analysis after filtering by call rate and missing data, in total 1,233 markers. The maximum genetic distance between isolate SG1 replicate sample controls was determined to be 0.0085, which was used to contract the number of MLGs. This yielded 338 individual MLGs from 346 *Ptm* isolates: 276 were Australian, 12 Canadian, 15 from the RSA, 10 Hungarian, 24 Turkish, and a single MLG from a historical Danish-type isolate. No MLGs were shared among countries or between regions within a country, and only four MLGs were composed of more than one isolate. These were predominantly from the more intensively sampled sites in Western Australia, with 3 groups involving 10 isolates, and 1 group of 2 isolates from Proteum in the RSA.

### Genetic diversity and differentiation between countries

Nei's unbiased gene diversity ranged from 0.13 to 0.25, averaging 0.20 (Table 1). Isolates from Turkey had the highest diversity, and those from Australia and Hungary had the lowest. The corrected Simpson's index, which indicates the probability that two randomly selected isolates in a population have a different genotype, suggested high MLG diversity for all populations ( $1 - \lambda > 0.99$ ). This is supported by low standardized index of association ( $\bar{r}_d$ ) values, ranging from 0.010 to 0.043, suggesting predominantly sexual reproduction, with the exception of Turkish isolates, with a value of 0.176. This higher value may be due to population substructure, which increases genome-wide linkage disequilibrium

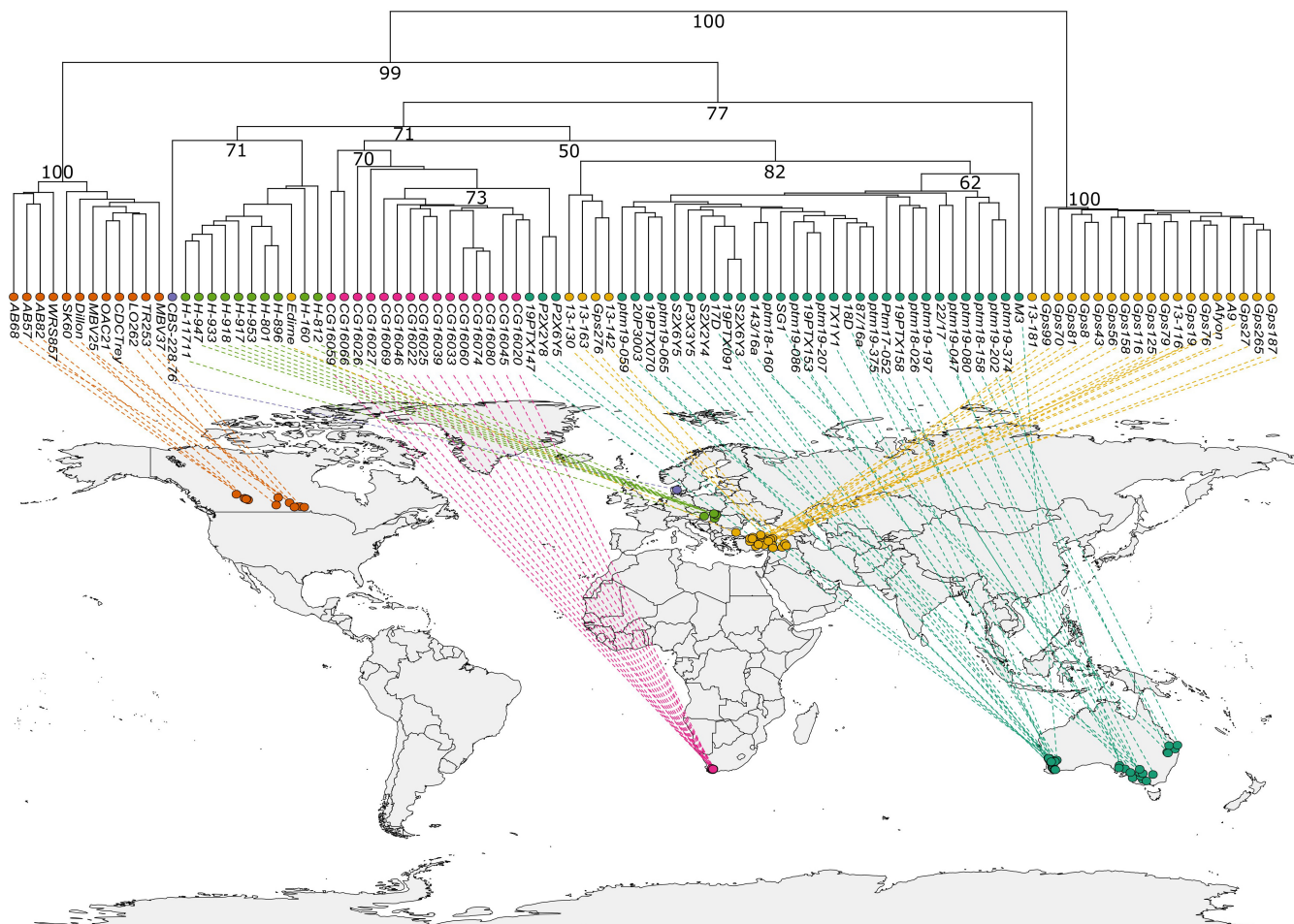


**Fig. 1.** Genetic relationships between *Pyrenophora teres* f. *maculata* (*Ptm*) isolates and their collection locations. The dendrogram is based on Prevosti's distance model (Prevosti et al. 1975) using DArTseq data for isolates from Australia ( $n = 34$ , in cyan), Canada ( $n = 12$ , orange), Denmark ( $n = 1$ , purple), the Republic of South Africa ( $n = 15$ , deep pink), Hungary ( $n = 10$ , green), and Turkey ( $n = 24$ , yellow). Bootstrap support values above 50% are shown at major branch points.

estimates both theoretically (Li and Nei 1974) and empirically (Andolfatto and Przeworski 2000; Browning and Browning 2011), influenced by genetic bottlenecks, the mixing of individuals between subpopulations that have different allele frequencies and where selfing or inbreeding is prevalent (Slatkin 2008; Wright et al. 2003).

Analysis of molecular variance of the entire clone-corrected data showed significant genetic differentiation of *Ptm* isolates ( $P < 0.01$ ) both within and among countries, with 53% of the genetic variation occurring among countries and 47% occurring within (Supplementary Table S3). Differentiation among regions within countries was not significant except in Turkey (67.17%;  $P < 0.01$ ). Pairwise population differentiation as defined by PhiPT was highest between Australian and Canadian populations (0.58), followed by Australian and Turkish populations, and lowest between the Australian and RSA populations (0.34; Supplementary Table S4).

### Genetic relationships between *Ptm* isolates based on genetic distance

A phylogenetic dendrogram based on Prevosti's genetic distance model (Prevosti et al. 1975) was produced using a subset of the Australian isolates, as well as all isolates from the other countries (Fig. 1). The dendrogram showed clustering based on country of origin with a few exceptions that were consistent with the PCA, DAPC, and STRUCTURE results below. The Turkish isolates from Central Anatolia were the most distant from all other isolates, whereas isolates from the southeastern Turkey group were closest to the Australian isolates. The tree also showed that a Turkish isolate, 'Edirne', from Edirne Province, which is on the European side of the Turkish Straights, was most similar to the Hungarian isolates. One Turkish isolate, 13-181, formed an outgroup to branches leading to the Australian, Hungarian, and RSA isolates. This contrasted with Gps 276, collected from *H. bulbosum*, which grouped with Turkish *H. vulgare* isolates sharing a branch with Australian isolates, suggesting an overlapping host range. Several Australian isolates shared a common branch with the RSA isolates, and isolate M3 was the most diverged, branching outside of the main group and supporting the STRUCTURE cluster membership allocation described below. The single Danish-type isolate (CBS 228.76) did not group with Hungarian isolates, lying between these and the Canadian clade.

### Principal components and multivariate clustering analyses

The genetic relatedness of all 338 MLGs was assessed by PCA and DAPC, an unsupervised multivariate clustering method used to assign isolates to groups of related individuals without a priori assumptions. Both approaches provided similar results to the distance-based analysis. The first two PCA components explained

17.9 and 6.2% of the variation (Supplementary Fig. S1) and assigned most isolates to their countries of origin, although a proportion occupied intermediate positions between 95% confidence ellipses ( $n > 25$ ). DAPC suggested models of between four and six clusters (Supplementary Fig. S2), with  $K = 5$  as the optimal value for subsequent analysis. More isolates were assigned to their host countries than PCA, particularly for isolates from Hungary, Canada, and Turkey (Supplementary Fig. S3). However, six Turkish isolates and the Danish-type isolate noticeably grouped with the Hungarian isolates, indicating the existence of related alleles (Jombart et al. 2010), and one RSA isolate grouped with the Canadian cluster. Most of the Australian isolates formed a single cluster, and 11 isolates from Western Australia grouped with RSA isolates, as opposed to only two assigned by PCA. These were the same isolates identified as an outgroup in a previous study by Hassett et al. (2023).

### Model-based clustering analysis

The Bayesian-inference program STRUCTURE was also used to assign genetic groupings, based on an optimal number of two clusters determined by STRUCTURE HARVESTER (Supplementary Fig. S4). At this level of differentiation, the Australian isolates belonged to a single cluster, and most isolates from Turkey were placed within the second cluster (Fig. 2). Isolates from the RSA, Hungary, and Canada showed mixed origin. Using a 70% cutoff score to assign isolates to a single cluster, all Australian, most RSA ( $n = 14$ ), most Hungarian ( $n = 6$ ), and most Turkish isolates from the southeast of the country ( $n = 5$ ) grouped into Cluster I, whereas only Turkish isolates from Ankara, the Black Sea, and Eastern regions formed Cluster II (collectively termed Central Anatolian isolates). All Canadian isolates, a single RSA isolate, four Hungarian isolates, the single Danish isolate, and a Turkish isolate showed intermediate membership of both clusters.

In common with the PCA and DAPC results, population structure by country was visible in the STRUCTURE results up to  $K = 5$ . Australian isolates appeared to be composed of mixed origin, with a larger primary cluster and a smaller admixed group. Isolates with membership to the admixed group ( $n = 8$ , cutoff  $> 50\%$ ) were made up of a similar subgroup identified in the DAPC results as being closer to the RSA population. Additional distinctive isolates found only in Western Australia included M3 and M4, collected from the same location in 2009, which appear to share modest and different membership proportions (cutoff  $> 5\%$ ) with Hungary and the RSA, despite belonging to the main Australian population.

### Fungicide resistance status of Australian, RSA, and Turkish isolates

Tebuconazole, a widely used representative of the DMI group of fungicides, was used in discriminatory dose screens to compare resistance phenotypes. The tests were performed on a selection of West Australian isolates that clustered with the RSA isolates, referred to as RSA-like, contained within the DAPC subset and at  $K = 4$  in STRUCTURE with an RSA similarity Q-score of more than 0.20 ( $n = 14$ ), the 2016 RSA isolates ( $n = 14$ ), randomly selected isolates from the primary Australian DAPC cluster ( $n = 29$ ), and a selection of Turkish isolates ( $n = 4$ ). Additional screens showed that the Turkish isolates were sensitive to tebuconazole (data not shown), and four were selected from groupings based on genetic distance (Fig. 1). Two (Gps43 and Gps76) were from Central Anatolia, representing the group of isolates most distant from all other isolates. The remaining two were from Southeastern Anatolia, with one (13-163) belonging to a clade next to the Australian isolates and the second (13-181) representing an outgroup to isolates from Australia, the RSA, and Europe. All the RSA-like isolates were HR, with the exception of isolate M3. Approximately half of the Australian primary cluster isolates were moderately resistant (MR,  $n = 14$ ), and the remainder were sensitive ( $n = 15$ ). Most 2016 RSA isolates ( $n = 12$ ) were HR, with two MR, whereas the Turkish isolates were sensitive (Supplementary Table S5).

TABLE 1. Genetic diversity indices for groups of *Pyrenophora teres* f. *maculata* isolates from five countries based on DaRTseq data<sup>a</sup>

Country	<i>n</i>	MLG	eMLG	<i>H</i>	$1 - \lambda$	$H_{exp}$	$\bar{r}_d$
Australia	283	276	9.98	5.6	1.000	0.144	0.010
Canada	12	12	10	2.48	1.000	0.156	0.010
RSA	16	15	9.62	2.69	0.992	0.163	0.043
Hungary	10	10	10	2.3	1	0.131	0.030
Turkey	24	24	10	3.18	1.000	0.248	0.176
Total	346	338*	9.99	5.82	1.000	0.204	0.081

<sup>a</sup> The indices were generated using the *poppr* function within *poppr* v 2.8.3 (Kamvar et al. 2014). *n*: number of isolates in each sample group. MLG: The total number of unique multilocus genotypes (MLGs) from each country. \*Total includes a single MLG from Denmark. eMLG: the expected number of MLGs. *H*: Shannon-Wiener index of MLG group genotypic diversity, a measure of the number of unique genotypes and their homogeneity.  $1 - \lambda$ : corrected Simpson's index of MLG diversity, the probability two isolates from the same dataset are different genotypes.  $H_{exp}$ : Nei's unbiased gene diversity index, the probability that two randomly selected alleles are different.  $\bar{r}_d$ : the standardized index of association, with a value of zero for a null hypothesis a population is freely recombining. RSA: Republic of South Africa.

### *Ptm Cyp51a* gene sequence comparisons

Mair et al. (2020) previously studied *Ptm* fungicide sensitivity and *Cyp51A* gene sequences in Western Australia and described five *Cyp51A* SNP-based haplotypes (H1 to H5). DMI-sensitive isolates were present in H1 and H2, with H2 also containing MR1 isolates, defined as containing a long terminal repeat (LTR) retrotransposon-like promoter insertion element and being moderately resistant to tebuconazole and resistant to epoxiconazole. HR isolates were found in H3 and H4 haplotypes, whereas H5 contained MR2 isolates, defined as being moderately resistant to tebuconazole but sensitive to epoxiconazole. DMI resistance in H3, H4, and H5 was due to three different F489L mutations: c1467a, c1467g, and t1465c, respectively.

To investigate *Cyp51A* variants, the gene and 846 bp upstream of the start codon was sequenced for 95 isolates. These included all the isolates used in the tebuconazole screens described above, as well as the 24 RSA isolates collected in 2007 and eight Hungarian isolates. Single representatives of haplotypes H3 and H5 from Mair et al. (2020) were also included, as they were not detected among our samples.

*Cyp51A* had 26 SNPs across the collection. Excluding F489L mutations, eight were non-synonymous substitutions. Of these, six were exclusive to the Turkish isolates and two to the Australian isolates. Three codon variants led to the nonsynonymous F489L mutation, and, consistent with Mair et al. (2020), all HR isolates contained both the mutation and a *Ty1-Copia* LTR retrotransposon-like insertion in the promoter, whereas all sensitive isolates had the wild-type codon. Moderately resistant isolates also either possessed the F489L mutation or contained a transposon insertion alone. Most Hungarian isolates ( $n = 7$ ) and all the 2007 RSA isolates contained the F489L mutation (data summarized in Supplementary Table S5).

H1 and H2 haplotypes were found only in Australian isolates. H1 was represented by 27 isolates but H2 only by a single isolate, M3. This isolate was collected from the same location as the specimen identified in Mair et al. (2020), suggesting a local variant. The second most common Australian haplotype was H4 with 13 isolates. Thirteen *Ptm Cyp51A* haplotypes additional to those in the Mair et al. (2020) study were found and numbered consecutively (H6 to H18). These are defined in Supplementary Table S6, with alignments provided in Supplementary File S1. The sequences are available in GenBank under accessions OR734722 to OR734732 and OR751399 to OR751400. Most were composed of single isolates including haplotype H6 with Australian isolate S2X2Y4, H7 with Hungarian isolate H801, and H8 with Turkish isolate 13-181. H11 and H17 contained the 2007 RSA

isolates PTM55 and PTM57, respectively. H14 contained Hungarian isolate H812, whereas H15, H16, and H18 contained Turkish isolates GPS76, 13-163, and GPS43, respectively. More common haplotypes included H9, with isolates from both the 2007 RSA ( $n = 19$ ) and 2016 RSA ( $n = 8$ ) collections. H10 included an isolate from Australia, P3X2Y9, and two isolates from the RSA 2016 collection. H12 contained most of the Hungarian isolates ( $n = 6$ ). H13 comprised isolates from both the 2007 ( $n = 2$ ) and the 2016 RSA collections ( $n = 3$ ).

A minimum spanning network of the *Cyp51A* gene was produced to illustrate haplotype relationships and their fungicide resistance status (Fig. 3). Close relationships were apparent between Australian and RSA isolates: haplotype H4, which included one putatively HR isolate from the 2007 RSA collection (PTM24), one HR isolate from the 2016 RSA collection (CG16045), and all 13 HR RSA-like Australian isolates; haplotype H10, which contained

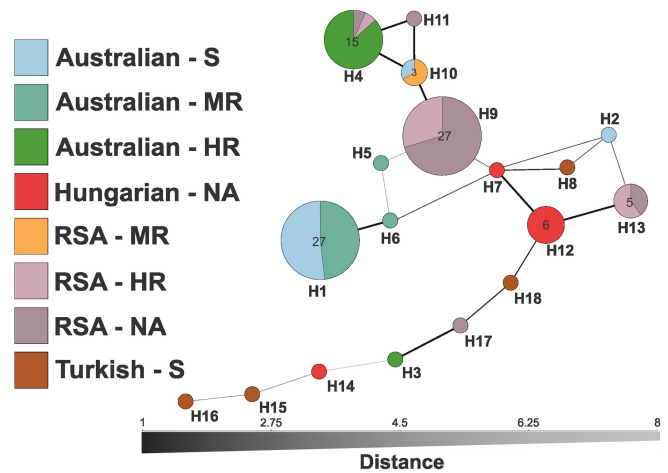
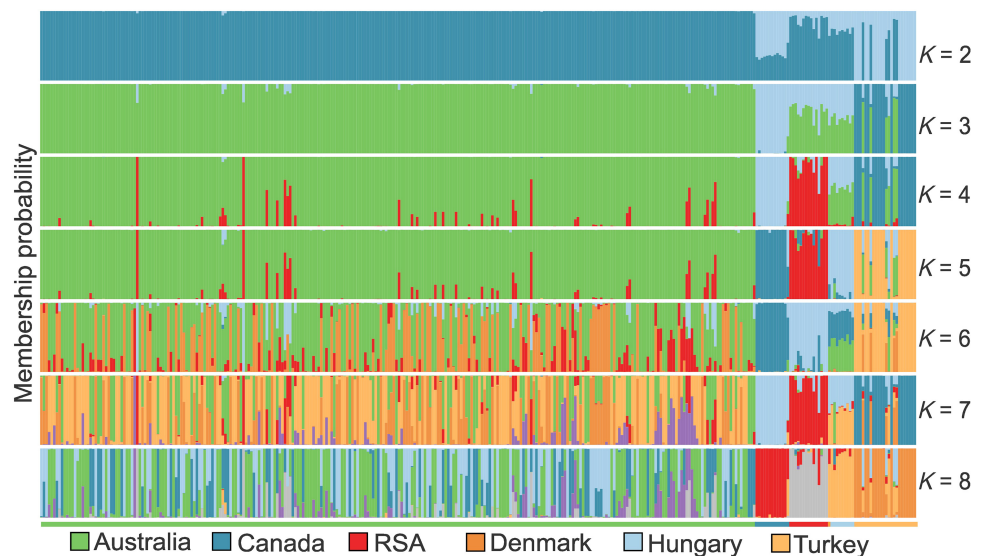


**Fig. 3.** Minimum spanning network based on *Pyrenophora teres* f. *maculata* *Cyp51A* gene sequences comparing international haplotype relationships. Each circle (node) represents a unique haplotype of *Cyp51A*, and each node size is proportional to the number of sampled isolates. Isolate origins and fungicide phenotypes are presented as proportionate sectors of nodes with wider and darker lines between nodes representing higher genetic relatedness. HR, MR, S, and NA indicate highly resistant, moderately resistant, and sensitive isolate responses to tebuconazole or data not available, respectively. Single representative sequences for H3 and H5 were obtained from Mair et al. (2020). RSA: Republic of South Africa.

**Fig. 2.** Estimates of genetic structuring in the entire clone-corrected *Pyrenophora teres* f. *maculata* (*Ptm*) collection grouped into clusters ( $K = 2$  to 8) in STRUCTURE. The colored bar at the base of the figure represents isolates grouped by country from Australia ( $n = 276$ ), Canada ( $n = 12$ ), Republic of South Africa (RSA;  $n = 15$ ), Denmark ( $n = 1$ ), Hungary ( $n = 10$ ), and Turkey ( $n = 24$ ), respectively. Vertical bars represent individual isolates, and the color proportions in each bar indicate the estimated membership fraction of each individual to each cluster.



two MR RSA isolates and one Australian sensitive isolate; and Australian HR haplotype H3 and H17 from RSA (untested) were also closely related. Several RSA isolates from 2007 ( $n = 3$ ) and 2016 ( $n = 2$ ) in H13 showed a strong relationship with most of the Hungarian isolates ( $n = 6$ ) in H7 and H12, reflecting DArTseq-based PCA and genetic distance-based proximities.

### ***Ptm Cyp51a* promoter region polymorphisms**

Sequence data of the promoter region of *Cyp51A* revealed 32 SNPs and six haplotypes. P1 and P2 were reported by Mair et al. (2020), and four new, predominantly Turkish haplotypes, P3 to P6, are novel to this study. A minimum spanning network (Supplementary Fig. S5), excluding transposon insertions (see below), shows that all tebuconazole HR *Cyp51A* haplotypes were found within node P2, MR isolates were located within P1 and P2, and sensitive isolates were found in all six nodes. As with the *Cyp51A* gene haplotypes, the Turkish sequences are the most diverged. An alignment of P1 to P6 is provided in Supplementary File S2, and P3 to P6 sequences are available in GenBank under accessions OR734240, OR734248, OR734250, and OR734251.

Five different LTR transposon variants were found within the upstream region of *Cyp51A* in the P1 and P2 haplotypes, defined by different combinations of three SNPs. Twelve independent insertion events in the two haplotypes were observed, with insertion of different alleles at two positions giving a total of 14 different transposon variant and location combinations (Supplementary File S3). We propose a new naming convention to account for different transposon alleles at the same position, which is presented together with GenBank accession numbers in Supplementary Table S7. In essence, the names are based on the two backbone haplotypes from which all mutations conferring resistance are derived (P1 and P2), followed by the promoter transposon insertion position relative to the *Cyp51A* start codon, then the *Ty1*-Copia LTR retrotransposon-like insertion allele number. The more notable of these include P2:90:1 and P2:95:2, which are present in HR isolates from Australia and the RSA and with one RSA isolate, PTM24, possessing the same *Cyp51A* F489L codon found in Australia; P2:46:5, which is shared between Australian and Hungarian isolates; and MR isolates from Australia, which have unique transposon insertion haplotypes (Supplementary Table S5).

A dendrogram combining all *Cyp51A* gene and promoter sequence data together with promoter transposon insertion sites and *Cyp51A* 489 codon usage was produced to summarize and distinguish the interrelationships of variants (Fig. 4). The figure illustrates the range of unique transposon insertion sites in combination with F489L mutations present in *Ptm* and highlights the key divergence point between the P1 and P2 base promoter haplotypes, which separates P2 predominantly HR isolates (containing both F489L mutations and transposon insertions) from P1 MR isolates (containing transposon insertions only) and S isolates. The RSA isolates possessed the largest number of P2 transposon insertion alleles (seven), which may indicate selection over a longer period. This is compared with three in Australian P2 isolates, followed by four for Australian P1 isolates. The only completely identical SNP and insertion profile (H4-P2:90:1) found between countries is boxed in blue and depicts the 2007 RSA isolate PTM24 and most of the Australian HR isolates.

## **Discussion**

Human trading and cultivation activities have profoundly impacted the distribution and dispersal of plant pathogens, a process that has accelerated in the current era of globalized transport (Bebber et al. 2014; Sotiropoulos et al. 2022). In this study, we examined genetic relationships between *Ptm* isolates in the most geographically widespread collection assembled to date. Preexisting genotyping data for Western Australian isolates formed most of the collection and, based on Nei's unbiased gene diversity index,

served as a control to show that deeper sampling does not necessarily improve the detection of general regional diversity; however, a few unusual localized patterns were revealed. Overall, the results revealed population subdivision related to country of origin and, with the exception of Turkey, similar amounts of diversity within countries as among countries. Regional selection of *Ptm* was evident, particularly of fungicide resistant isolates, and evidence for admixturing of isolates between the RSA and Australia. These results contrast with *Ptt*, which shows greater admixturing of genotypes between countries and deep phylogenetic lineages at the whole-genome level (Dahanayaka et al. 2021b; Moolhuijzen et al. 2020), perhaps reflecting a longer association with barley (Ellwood et al. 2012).

### **Intercontinental *Ptm* population subdivision**

Principal components, genetic distance, and STRUCTURE-based analyses indicated that Turkish isolates from Central Anatolia showed distinct separation from all other isolates, whereas Canadian isolates were also placed in a discrete cluster. Isolates from Australia and the RSA were closely related; however, all the analyses supported *Ptm* population subdivision related to country of origin. The greater differentiation of Canadian isolates may be due to adaptation to a distinctive subgroup of barley genotypes (Hill et al. 2021) or a bottleneck effect and/or genetic drift during initial establishment. Australia and the Western Cape of the RSA share similar environments and climates, which may have driven the selection of common genotypes, as well as a history of shared cultivars, such as Clipper (Campbell and Crous 2002).

The methods above also indicated several isolates with uncertain ancestry, either falling between principal component 95% confidence ellipses or occupying unexpected positions in the distance-based tree and evidence for admixed individuals in STRUCTURE. DAPC, a multivariate approach that quantifies the contribution of individual alleles to population structuring (Jombart et al. 2010), provided clearer allocation of these individuals to genetic groupings, placing 11 of 276 of the Australian isolates with the RSA group, one RSA isolate with the Canadian group, and six Turkish isolates and the single Danish isolate into the Hungarian group. However, the DAPC results also indicated a few isolates with ambiguous placements that may represent recent migration events, membership of unsampled populations, or uncommon genotypes. For example, two of the six Turkish isolates lay outside of the Hungarian group's 95% confidence ellipse, as well as the RSA isolate placed with Canadian isolates.

A Turkish isolate from Edirne was closely related to the Hungarian isolates, a result confirmed by sequence data for a unique effector gene haplotype in Europe (J. Lawrence and S. R. Ellwood, unpublished data). This may be explained by the sampling location, as Edirne lies on the western side of the Turkish Straights, a body of water separating Eastern Thrace, a province of Turkey in southern Europe, and Anatolia. Such a physical barrier may limit dispersion and the exchange of genetic material. The grouping of this isolate, the Danish isolate, and those from Hungary suggests modest genetic variation across Europe, although the sample size was low.

### **High genetic diversity and population substructure in Turkey**

Turkish *Ptm* isolates from Central Anatolia showed greater genetic distances from all other isolates. Regional genotypic clustering was observed, a phenomenon not present among isolates from the other countries in this study, with Central Anatolian isolates grouping separately from Southeastern Anatolian and the Edirne isolate, which are more closely related to the globally distributed populations. This structuring may reflect host selection on the diverse barley genotypes found in Turkey within different environmental niches, as Turkey lies along the northern extent of the Fertile Crescent (Breasted 1916), which is believed to be the first region where barley was domesticated (Zohary and Hopf 2000) and a major center of diversity (Dai et al. 2012; Orabi et al. 2007).

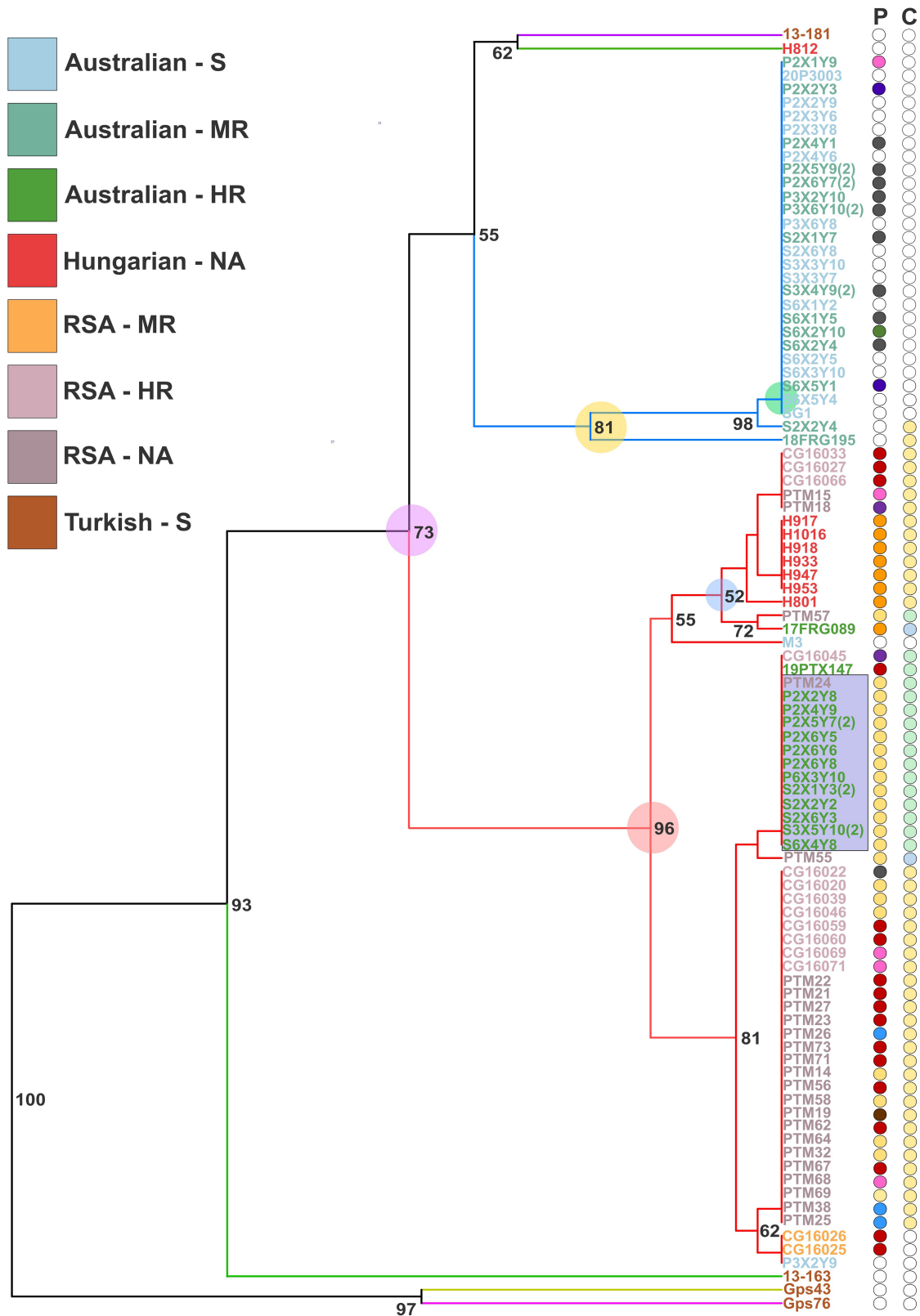


**Fig. 4.** Phylogram of *Pyrenophora teres* f. *maculata* relationships based on *Cyp51A* promoter and gene sequences and transposon insertion data. The dendrogram is based on 71 possible differences (58 single-nucleotide polymorphisms and 14 different transposon allele insertion position combinations). Colored branches indicate divergence events leading to six basal promoter variants in Supplementary Figure S5. The node depicted in purple shows the key branch point separating P1 from P2 isolates (depicted by the yellow and red nodes, respectively). The blue node highlights a transposon insertion found in the Hungarian isolates and the highly resistant (HR) Australian 17FRG089 H3-P2:46:5 haplotype. The green node depicts the point past which two new transposon insertions occur in the P1 haplotype of the Australian population (indicated by the dark green and dark blue circles in the promoter column). The boxed isolates contain identical haplotypes from Western Australia and the Republic of South Africa (RSA). Full haplotype pedigrees are provided in Supplementary Table S5. P indicates promoter transposon insertion position: white, no insertion; orange, -46; brown, -57; light blue, -62; pink, -66; gray, -74; dark blue, -75; green, -77; yellow, -90; purple, -94; and red, -95. C represents the *Cyp51A* 489 codon nucleotide sequence: white, TTC (wild type); yellow, CTC; green, TTG; and blue, TTA. HR, MR, S, and NA indicate highly resistant, moderately resistant, and sensitive isolate responses to tebuconazole or data not available, respectively. Bootstrap support values above 50% are shown for major branch points.



There are significant climatic differences and changes in elevation between Turkish regions, with Southeastern Anatolia having some of the hottest summers, compared with the coolest found in the western Marmara (Sensoy 2004). Aside from wild barley species such as *Hordeum spontaneum* and *H. bulbosum* (Karakaya et al. 2016, 2020), winter-sown feed barley cultivars are common in Turkey (Sipahi et al. 2010), and landraces with purple or black grain are grown extensively, particularly in Southeastern Turkey (Ozberk et al. 2020). The southeastern isolates, or other unsampled populations along the Fertile Crescent, might be regarded as the source of closely related genotypes in Australia and elsewhere, or alternatively represent migration to Turkey via introduced modern cultivars.

Çelik Oğuz et al. (2019) previously assessed genetic similarities of 49 Turkish *Ptm* isolates and found two main groups but no link between sampling year, mating type, or geographical area. In neighboring Iran, Vasighzadeh et al. (2021) found strong population structure among 116 isolates, with most of the genetic variation contained within regional populations. Those studies used different types of genetic markers and different PCR product resolution methods (anonymous inter-SSRs resolved by agarose gel electrophoresis and SSRs separated on a sequencing platform, respectively). SSR markers are more similar to DArT markers in terms of detecting specific loci and higher numbers of sequence polymorphisms per individual, which limits comparisons with inter-SSRs, although, complimentary to this study, Çelik Oğuz et al. (2019) found that isolates from Central Anatolia formed the majority of one of their groups.

#### Fungicide-resistant Western Australian *Ptm* isolates share genetic similarities with RSA isolates

Hassett et al. (2023) identified a “cryptic” group of Western Australian isolates by DAPC, with no obvious association with geographic distance or host cultivar. Examination of genes contributing to differentiation implicated the *Cyp51A* gene, mutations of which underlie resistance to the DMI Group 3 triazole fungicides. DMI fungicides act through C14 $\alpha$ -demethylase to inhibit ergosterol biosynthesis, an essential fungal plasma membrane component (Aoyama et al. 1996; Parks and Casey 1995; Yoshida 1993) and mutation of phenylalanine (F) to Leucine (L) at codon 489 (F489L) is the primary mechanism of resistance in *P. teres* (Mair et al. 2016, 2020).

In this study, admixture between the same Western Australian isolates and RSA isolates was indicated by DAPC, with support by STRUCTURE population membership assignments at  $K = 4$ . The STRUCTURE assignments indicated that these isolates possess varying proportions of the donor genome. Ellwood et al. (2019) discovered that rapid recombination occurred around a new *Ptt Cyp51A* resistance mutation in Western Australian individuals from the wider population some 2 years after initial reports, indicating the potential for rapid assimilation that may obscure the phylogenetic origin. To further explore their association, the RSA-like Western Australian and RSA isolates were studied by sequencing their *Cyp51A* gene and in experiments measuring resistance to the DMI tebuconazole. The RSA-like Australian isolates were HR, whereas the RSA isolates were MR to HR.

Mair et al. (2020) found that a combination of the *Ptm Cyp51A* F489L mutation together with a *Ty1-Copia* LTR retrotransposon-like insertion in the promoter correlated with constitutive *Cyp51A* overexpression to give an HR phenotype to different DMIs. When either the insertion element or the F489L mutation was absent, an MR phenotype was observed, and genotypes with neither mutation had a sensitive phenotype. In this study, no new non-synonymous F489L mutations were discovered among RSA and Australian isolates, and the same relationship between F489L, transposon insertion site, and phenotype was observed. However, new transposon alleles distinguished by SNP changes and their insertion sites were

identified in both the Australian and RSA populations, with an identical variant (H4-P2:90:1) shared between them. Furthermore, clustering of the promoter insertions in an approximately 50-bp region close to the start codon was evident, which may indicate disruption of a transcription repressor site, with counter-selection across the remaining 5' region underlining the importance of *Cyp51A* as an essential sterol synthesis gene.

Compromised *Ptm* sensitivity to a range of DMIs was reported in RSA isolates from the Western Cape collected between 1996 and 1997, including against tebuconazole (Campbell and Crous 2002). The authors commented that selection for fungicide resistance was likely promoted by extensive cultivation at the time of Clipper, a cultivar susceptible to spot form net blotch. Most of the isolates appear to have been either S or MR based on the fungicide concentrations tested, but at least one isolate possessed an IC<sub>50</sub> (half maximal inhibitory concentration) of more than 20  $\mu\text{g ml}^{-1}$  tebuconazole, suggesting that HR isolates have existed since 1997. Genetic similarities of the RSA-like Western Australian isolates together with high levels of preexisting tebuconazole resistance in RSA isolates indicates either similar ancestry or an event enabling inter-crossing between the two populations. Convergent evolution leading to these isolates may be also be an explanation. However, the existence of the RSA-like Western Australian subgroup isolates only in recent collections and their different RSA-like membership proportions detected in STRUCTURE would argue against this possibility.

#### Multiple independent DMI fungicide resistance events

Hungarian *Ptm Cyp51A* haplotypes grouped together in a single phylogenetic cluster, and most contained non-synonymous F489L mutations and a transposon insertion in the promoter, indicating high levels of tebuconazole resistance which are known to exist in European isolates (Lammari et al. 2020). However, promoter insertions for all the Hungarian isolates were at -46 bp before the start codon, a site not found in the RSA isolates but indicating mechanistic convergent evolution for enhanced DMI resistance.

The only known instance of the -46 bp transposon outside of Hungary was found by Mair et al. (2020) in the HR Western Australian haplotype H3-P2:46:5. Nevertheless, there were differences in SNP composition within the *Cyp51A* gene and in the F489L codon (t1465c for Hungarian isolates and c1467a for H3 isolates). No H3 genotypes were detected in this study, but it is worth noting they were not found among Australian isolates prior to 2017, with almost all collected from heavily infected cultivar Oxford plants in southwestern Western Australia (Mair et al. 2020). This suggests an association with cultivar-specific enhanced virulence that has become uncommon, as cultivar Oxford is no longer recommended in sowing guides. The RSA-like HR isolates, by contrast, were almost entirely sampled north of Perth, confirming independent regional emergence of fungicide resistance.

Two groups of RSA isolates were used in this study, recent (post-2016) and those from 2007. We were unable to measure resistance in the 2007 isolates, as only their DNA was available, but isolates with matching gene and promoter mutations among the 2016 isolates were screened, which indicated that the older isolates were likely HR to DMI fungicides. Several haplotypes from the 2007 RSA population were absent in the more modern population, but they too contained a promoter insertion and F489L mutation, suggesting that they were also HR. Notably, H4 isolates, which included representatives of the RSA-like Australian isolates, a 2007 RSA isolate, and a 2016 RSA isolate, all had identical *Cyp51A* gene sequences, further indicating the similarity of isolates from these regions.

The appearance of different *Cyp51A* F489L mutations and promoter transposon insertions in different *Ptm* populations is an example of convergent evolution. However, there is also evidence of “soft selective sweeps,” a phenomenon whereby multiple alleles at the same locus, present either in standing genetic variation or

generated during selection, become prevalent (Delmas et al. 2017; Hermisson and Pennings 2005). The RSA 2007 isolates possessed three separate F489L mutation alleles, suggesting at least three independent gains of DMI resistance, whereas multiple examples of different transposon insertions are evident within the Western Australia and RSA populations (Fig. 4). The global appearance of these different mutations illustrates how *Ptm* readily generates DMI resistance, seemingly without relying on target site duplications as found in *Ptt*, for which promoter insertions have not been reported (Mair et al. 2016; Turo et al. 2021).

This study provides a baseline of current *Ptm* genotypic diversity between countries and suggests the pathogen has a defined population structure at the international level that is consistent with a model of recent introductions involving genetic bottlenecks and drift with adaptation to new environments. Turkish isolates were the most genetically diverged, with regional sub-structuring and with some individuals genetically similar to isolates from other countries. The Turkish isolates also showed the largest number of SNPs in the *Cyp51A* gene and phylogenetically contain the most diverged individuals compared with all other samples in this study. However, they were sensitive when challenged with tebuconazole, which aligns with traditional cultivation practices without fungicides. The Australian population appeared autonomous except for a subgroup with genetic similarities to RSA isolates with which they shared similar *Cyp51A* gene and promoter region changes conferring DMI fungicide resistance, suggesting a shared origin of resistance. The range of *Ptm* genotypes uncovered in this study will aid future research investigating host–pathogen interactions for this significant crop disease.

#### Acknowledgments

We thank Sandra Lamprecht and Yared Tewoldemedhin (Agricultural Research Council, Republic of South Africa), Driecus Lesch (Sensako Pty Ltd), Daniel De Klerk (South African Barley Breeding Institute), and Elsabet Wessels and Corneli Smit (CenGen) for assistance with sample collection of the RSA isolates. We also thank Wesley Mair for fungicide resistance guidance. Research activities were undertaken with the support of Australian grain producers within the Centre for Crop and Disease Management, a co-investment of Grains Research and Development Corporation (GRDC) and Curtin University, under GRDC CUR00023 B3.2.

#### Literature Cited

- Agapow, P.-M., and Burt, A. 2001. Indices of multilocus linkage disequilibrium. *Mol. Ecol. Notes* 1:101-102.
- Ahmed Lhadj, W., Boungab, K., Righi Assia, F., Çelik Oğuz, A., Karakaya, A., and Ölmez, F. 2022. Genetic diversity of *Pyrenophora teres* in Algeria. *J. Plant Pathol.* 104:305-315.
- Akhavan, A., Turkington, T. K., Kebede, B., Tekauz, A., Kutcher, H. R., Kirkham, C., Xi, K., Kumar, K., Tucker, J. R., and Strelkov, S. E. 2015. Prevalence of mating type idiomorphs in *Pyrenophora teres* f. *teres* and *P. teres* f. *maculata* populations from the Canadian prairies. *Can. J. Plant Pathol.* 37:52-60.
- Akhavan, A., Turkington, T. K., Kebede, B., Xi, K., Kumar, K., Tekauz, A., Kutcher, H. R., Tucker, J. R., and Strelkov, S. E. 2016. Genetic structure of *Pyrenophora teres* f. *teres* and *P. teres* f. *maculata* populations from western Canada. *Eur. J. Plant Pathol.* 146:325-335.
- Andolfatto, P., and Przeworski, M. 2000. A genome-wide departure from the standard neutral model in natural populations of *Drosophila*. *Genetics* 156:257-268.
- Aoyama, Y., Noshiro, M., Gotoh, O., Imaoka, S., Funae, Y., Kurosawa, N., Horiuchi, T., and Yoshida, Y. 1996. Sterol 14-demethylase P450 (P45014DM) is one of the most ancient and conserved P450 species. *J. Biochem.* 119: 926-933.
- Bebber, D. P., Holmes, T., and Gurr, S. J. 2014. The global spread of crop pests and pathogens. *Glob. Ecol. Biogeogr.* 23:1398-1407.
- Bogacki, P., Keiper, F. J., and Oldach, K. H. 2010. Genetic structure of South Australian *Pyrenophora teres* populations as revealed by microsatellite analyses. *Fungal Biol.* 114:834-841.
- Breasted, J. H. 1916. *Ancient Times, a History of the Early World: An Introduction to the Study of Ancient History and the Career of Early Man.* Ginn and Company, Boston, MA.
- Browning, S. R., and Browning, B. L. 2011. Population structure can inflate SNP-based heritability estimates. *Am. J. Hum. Genet.* 89:191-193.
- Campbell, G. F., and Crous, P. W. 2002. Fungicide sensitivity of South African net- and spot-type isolates of *Pyrenophora teres* to ergosterol biosynthesis inhibitors. *Australas. Plant Pathol.* 31:151-155.
- Campbell, G. F., Lucas, J. A., and Crous, P. W. 2002. Evidence of recombination between net- and spot-type populations of *Pyrenophora teres* as determined by RAPD analysis. *Mycol. Res.* 106:602-608.
- Çelik Oğuz, A., Ölmez, F., and Karakaya, A. 2019. Genetic diversity of net blotch pathogens of barley in Turkey. *Int. J. Agric. Biol.* 21:1089-1096.
- Clare, S. J., Wyatt, N. A., Brueggeman, R. S., and Friesen, T. L. 2020. Research advances in the *Pyrenophora teres*–barley interaction. *Mol. Plant Pathol.* 21:272-288.
- Dahanayaka, B. A., Vaghefi, N., Knight, N. L., Bakonyi, J., Prins, R., Seress, D., Snyman, L., and Martin, A. 2021b. Population structure of *Pyrenophora teres* f. *teres* barley pathogens from different continents. *Phytopathology* 111: 2118-2129.
- Dahanayaka, B. A., Vaghefi, N., Snyman, L., and Martin, A. 2021a. Investigating in vitro mating preference between or within the two forms of *Pyrenophora teres* and its hybrids. *Phytopathology* 111:2278-2286.
- Dai, F., Nevo, E., Wu, D., Comadran, J., Zhou, M., Qiu, L., Chen, Z., Beiles, A., Chen, G., and Zhang, G. 2012. Tibet is one of the centers of domestication of cultivated barley. *Proc. Natl. Acad. Sci. U.S.A.* 109: 16969-16973.
- Delmas, C. E. L., Dussert, Y., Delière, L., Couture, C., Mazet, I. D., Richart Cervera, S., and Delmotte, F. 2017. Soft selective sweeps in fungicide resistance evolution: Recurrent mutations without fitness costs in grapevine downy mildew. *Mol. Ecol.* 26:1936-1951.
- Dray, S., and Dufour, A.-B. 2007. The ade4 package: Implementing the duality diagram for ecologists. *J. Stat. Softw.* 22:1-20.
- Earl, D. A., and von Holdt, B. M. 2012. STRUCTURE HARVESTER: A website and program for visualizing STRUCTURE output and implementing the Evanno method. *Conserv. Genet. Resour.* 4:359-361.
- Ellwood, S. R., Lopez-Ruiz, F. J., and Tan, K.-C. 2024. Barley powdery mildew control in Western Australia and beyond. *Plant Pathol.* <https://doi.org/10.1111/ppa.13884>
- Ellwood, S. R., Piscetek, V., Mair, W. J., Lawrence, J. A., Lopez-Ruiz, F. J., and Rawlinson, C. 2019. Genetic variation of *Pyrenophora teres* f. *teres* isolates in Western Australia and emergence of a *Cyp51A* fungicide resistance mutation. *Plant Pathol.* 68:135-142.
- Ellwood, S. R., Syme, R. A., Moffat, C. S., and Oliver, R. P. 2012. Evolution of three *Pyrenophora* cereal pathogens: Recent divergence, speciation and evolution of non-coding DNA. *Fungal Genet. Biol.* 49: 825-829.
- Falush, D., Stephens, M., and Pritchard, J. K. 2003. Inference of population structure using multilocus genotyped data: Linked loci and correlated allele frequencies. *Genetics* 164:1567-1587.
- Faris, J. D., and Friesen, T. L. 2020. Plant genes hijacked by necrotrophic fungal pathogens. *Curr. Opin. Plant Biol.* 56:74-80.
- Ge, C., Moolhuijzen, P., Hickey, L., Wentzel, E., Deng, W., Dinglasan, E. G., and Ellwood, S. R. 2020. Physiological changes in barley *mlo-11* powdery mildew resistance conditioned by tandem repeat copy number. *Int. J. Mol. Sci.* 21:8769.
- Ge, X., Deng, W., Lee, Z. Z., Lopez-Ruiz, F. J., Schweizer, P., and Ellwood, S. R. 2016. Tempered *mlo* broad-spectrum resistance to barley powdery mildew in an Ethiopian landrace. *Sci. Rep.* 6:29558.
- Hassett, K., Muria-Gonzalez, M. J., Turner, A., McLean, M. S., Wallwork, H., Martin, A., and Ellwood, S. R. 2023. Widespread genetic heterogeneity and genotypic grouping associated with fungicide resistance among barley spot form net blotch isolates in Australia. *G3* 13:jkad076.
- Hermisson, J., and Pennings, P. S. 2005. Soft sweeps: Molecular population genetics of adaptation from standing genetic variation. *Genetics* 169: 2335-2352.
- Hill, C. B., Angessa, T. T., Zhang, X.-Q., Chen, K., Zhou, G., Tan, C., Wang, P., Westcott, S., and Li, C. 2021. A global barley panel revealing genomic signatures of breeding in modern Australian cultivars. *Plant J.* 106: 419-434.
- Jaccoud, D., Peng, K., Feinstein, D., and Kilian, A. 2001. Diversity arrays: A solid state technology for sequence information independent genotyping. *Nucleic Acids Res.* 29:e25.
- Jeffries, D. L., Copp, G. H., Handley, L. L., Olsén, K. H., Sayer, C. D., and Hänfling, B. 2016. Comparing RADseq and microsatellites to infer complex phylogeographic patterns, an empirical perspective in the Crucian carp, *Carassius carassius*, L. *Mol. Ecol.* 25:2997-3018.
- Jombart, T. 2008. *adeigenet*: A R package for the multivariate analysis of genetic markers. *Bioinformatics* 24:1403-1405.
- Jombart, T., Devillard, S., and Balloux, F. 2010. Discriminant analysis of principal components: A new method for the analysis of genetically structured populations. *BMC Genet.* 11:94.

- Kamvar, Z. N., Tabima, J. F., and Grünwald, N. J. 2014. *Poppr*: An R package for genetic analysis of populations with clonal, partially clonal, and/or sexual reproduction. *PeerJ* 2:e281.
- Karakaya, A., Çelik Oğuz, A., and Saraç Sivrikaya, I. 2020. Diseases occurring on *Hordeum bulbosum* field populations at Bingöl province of Turkey. Pages 75-81 in: 30th International Scientific-Expert Conference of Agriculture and Food Industry Works of the Faculty of Agriculture and Food Sciences, University of Sarajevo, Sarajevo, Bosnia and Herzegovina.
- Karakaya, A., Mert, Z., Çelik Oğuz, A., Ertaş, M. N., and Karagöz, A. 2016. Determination of the diseases occurring on naturally growing wild barley (*Hordeum spontaneum*) field populations. Pages 291-295 in: 26th International Scientific-Expert Conference of Agriculture and Food Industry Works of the Faculty of Agriculture and Food Sciences, University of Sarajevo, Sarajevo, Bosnia and Herzegovina.
- Lammari, H.-I., Rehfus, A., Stammler, G., and Benslimane, H. 2020. Sensitivity of the *Pyrenophora teres* population in Algeria to quinone outside inhibitors, succinate dehydrogenase inhibitors and demethylation Inhibitors. *Plant Pathol. J.* 36:218-230.
- Lehmensiek, A., Bester-van der Merwe, A. E., Sutherland, M. W., Platz, G., Kriel, W. M., Potgieter, G. F., and Prins, R. 2010. Population structure of South African and Australian *Pyrenophora teres* isolates. *Plant Pathol.* 59:504-515.
- Li, W.-H., and Nei, M. 1974. Stable linkage disequilibrium without epistasis in subdivided populations. *Theor. Popul. Biol.* 6:173-183.
- Linde, C. C., and Smith, L. M. 2019. Host specialisation and disparate evolution of *Pyrenophora teres* f. *teres* on barley and barley grass. *BMC Evol. Biol.* 19:139.
- Liu, Z., Ellwood, S. R., Oliver, R. P., and Friesen, T. L. 2011. *Pyrenophora teres*: Profile of an increasingly damaging barley pathogen. *Mol. Plant Pathol.* 12:1-19.
- Lu, X., Kracher, B., Saur, I. M. L., Bauer, S., Ellwood, S. R., Wise, R., Yaeno, T., Maekawa, T., and Schulze-Lefert, P. 2016. Allelic barley MLA immune receptors recognize sequence-unrelated avirulence effectors of the powdery mildew pathogen. *Proc. Natl. Acad. Sci. U.S.A.* 113:E6486-E6495.
- Mair, W. J., Deng, W., Mullins, J. G. L., West, S., Wang, P., Besharat, N., Ellwood, S. R., Oliver, R. P., and Lopez-Ruiz, F. J. 2016. Demethylase inhibitor fungicide resistance in *Pyrenophora teres* f. sp. *teres* associated with target site modification and inducible overexpression of *Cyp51*. *Front. Microbiol.* 7:1279.
- Mair, W. J., Thomas, G. J., Dodhia, K., Hills, A. L., Jayasena, K. W., Ellwood, S. R., Oliver, R. P., and Lopez-Ruiz, F. J. 2020. Parallel evolution of multiple mechanisms for demethylase inhibitor fungicide resistance in the barley pathogen *Pyrenophora teres* f. sp. *maculata*. *Fungal Genet. Biol.* 145:103475.
- McDonald, B. A., and Linde, C. 2002. Pathogen population genetics, evolutionary potential, and durable resistance. *Annu. Rev. Phytopathol.* 40: 349-379.
- McLean, M. S., Howlett, B. J., and Hollaway, G. J. 2009. Epidemiology and control of spot form of net blotch (*Pyrenophora teres* f. *maculata*) of barley: A review. *Crop Pasture Sci.* 60:303-315.
- McLean, M. S., Martin, A., Gupta, S., Sutherland, M. W., Hollaway, G. J., and Platz, G. J. 2014. Validation of a new spot form of net blotch differential set and evidence for hybridisation between the spot and net forms of net blotch in Australia. *Australas. Plant Pathol.* 43:223-233.
- McLean, M. S., Poole, N., Santa, I. M., and Hollaway, G. J. 2022. Efficacy of spot form of net blotch suppression in barley from seed, fertiliser and foliar applied fungicides. *Crop Prot.* 153:105865.
- Melville, J., Haines, M. L., Boysen, K., Hodkinson, L., Kilian, A., Smith Date, K. L., Potvin, D. A., and Parris, K. M. 2017. Identifying hybridization and admixture using SNPs: Application of the DArTseq platform in phylogeographic research on vertebrates. *R. Soc. Open Sci.* 4:161061.
- Moolhuijzen, P., Ge, C., Palmiero, E., and Ellwood, S. R. 2023. A unique resistance mechanism is associated with *RBgh2* barley powdery mildew adult plant resistance. *Theor. Appl. Genet.* 136:145.
- Moolhuijzen, P. M., Muria-Gonzalez, M. J., Syme, R., Rawlinson, C., See, P. T., Moffat, C. S., and Ellwood, S. R. 2020. Expansion and conservation of biosynthetic gene clusters in pathogenic *Pyrenophora* spp. *Toxins* 12: 242.
- Muria-Gonzalez, M. J., Lawrence, J. A., Palmiero, E., D'Souza, N. K., Gupta, S., and Ellwood, S. R. 2023. Major susceptibility gene epistasis over minor gene resistance to spot form net blotch in a commercial barley cultivar. *Phytopathology* 113:1058-1065.
- Orabi, J., Backes, G., Wolday, A., Yahyaoui, A., and Jahoor, A. 2007. The Horn of Africa as a centre of barley diversification and a potential domestication site. *Theor. Appl. Genet.* 114:1117-1127.
- Ozberk, F., Ozberk, I., Ayhan, H., Bayhan, M., and Ipeksever, F. 2020. Marketing prices of barley in Southeastern Anatolia: Black vs. white hulled barley. *J. Agric. Sci. (Belgr.)* 65:297-310.
- Parks, L. W., and Casey, W. M. 1995. Physiological implications of sterol biosynthesis in yeast. *Annu. Rev. Microbiol.* 49:95-116.
- Peakall, R., and Smouse, P. E. 2012. GenAIEx 6.5: Genetic analysis in Excel. Population genetic software for teaching and research—An update. *Bioinformatics* 28:2537-2539.
- Peakall, R., and Smouse, P. E. 2006. GENALEX 6: Genetic analysis in Excel. Population genetic software for teaching and research *Mol. Ecol. Notes* 6: 288-295.
- Peters Haugrud, A. R., Zhang, Z., Richards, J. K., Friesen, T. L., and Faris, J. D. 2019. Genetics of variable disease expression conferred by inverse gene-for-gene interactions in the wheat–*Parastagonospora nodorum* pathosystem. *Plant Physiol.* 180:420-434.
- Poudel, B., Ellwood, S. R., Testa, A. C., McLean, M., Sutherland, M. W., and Martin, A. 2017. Rare *Pyrenophora teres* hybridization events revealed by development of sequence-specific PCR markers. *Phytopathology* 107: 878-884.
- Poudel, B., McLean, M. S., Platz, G. J., McIlroy, J. A., Sutherland, M. W., and Martin, A. 2019. Investigating hybridisation between the forms of *Pyrenophora teres* based on Australian barley field experiments and cultural collections. *Eur. J. Plant Pathol.* 153:465-473.
- Prevosti, A., Ocaña, J., and Alonso, G. 1975. Distances between populations of *Drosophila subobscura*, based on chromosome arrangement frequencies. *Theor. Appl. Genet.* 45:231-241.
- Pritchard, J. K., Stephens, M., and Donnelly, P. 2000. Inference of population structure using multilocus genotype data. *Genetics* 155:945-959.
- Rau, D., Brown, A. H. D., Brubaker, C. L., Attene, G., Balmás, V., Saba, E., and Papa, R. 2003. Population genetic structure of *Pyrenophora teres* Drechs. the causal agent of net blotch in Sardinian landraces of barley (*Hordeum vulgare* L.). *Theor. Appl. Genet.* 106:947-959.
- Revell, L. J. 2012. phytools: An R package for phylogenetic comparative biology (and other things). *Methods Ecol. Evol.* 3:217-223.
- Saghai Maroof, M. A., Biyashev, R. M., Yang, G. P., Zhang, Q., and Allard, R. W. 1994. Extraordinarily polymorphic microsatellite DNA in barley: Species diversity, chromosomal locations, and population dynamics. *Proc. Natl. Acad. Sci. U.S.A.* 91:5466-5470.
- Sánchez-Sevilla, J. F., Horvath, A., Botella, M. A., Gaston, A., Folta, K., Kilian, A., Denoyes, B., and Amaya, I. 2015. Diversity Arrays Technology (DArT) marker platforms for diversity analysis and linkage mapping in a complex crop, the octoploid cultivated strawberry (*Fragaria × ananassa*). *PLoS One* 10:e0144960.
- Sansaloni, C., Petrolì, C., Jaccoud, D., Carling, J., Detering, F., Grattapaglia, D., and Kilian, A. 2011. Diversity Arrays Technology (DArT) and next-generation sequencing combined: Genome-wide, high throughput, highly informative genotyping for molecular breeding of *Eucalyptus*. *BMC Proc.* 5:P54.
- Sensoy, S. 2004. The mountains influence on Turkey climate. Pages 1-10 in: Proceedings of the BALWOIS Conference on Water Observation and Information System for Decision Support. Balkan Water Observation and Information System, Ohrid, Macedonia.
- Serenius, M., Manninen, O., Wallwork, H., and Williams, K. 2007. Genetic differentiation in *Pyrenophora teres* populations measured with AFLP markers. *Mycol. Res.* 111:213-223.
- Shackley, B., Paynter, B., Bucat, J., Seymour, M., and Power, S. 2021. 2022 Western Australian crop sowing guide. Department of Primary Industries and Regional Development, State of Western Australia.
- Sipahi, H., Akar, T., Yıldız, M. A., and Sayim, I. 2010. Determination of genetic variation and relationship in Turkish barley cultivars by hordein and RAPD markers. *Turk. J. Field Crops* 15:108-113.
- Slatkin, M. 2008. Linkage disequilibrium - understanding the evolutionary past and mapping the medical future. *Nat. Rev. Genet.* 9:477-485.
- Smedegård-Petersen, V. 1971. *Pyrenophora teres* f. *maculata* f. nov. and *Pyrenophora teres* f. *teres* on barley in Denmark. Pages 124-144 in: Aarsskrift Kongelige Veterinær og Landbohøjskole. Aug. Bangs Boghandel, Copenhagen.
- Sotiropoulos, A. G., Arango-Isaza, E., Ban, T., Barbieri, C., Bourras, S., Cowger, C., Czembor, P. C., Ben-David, R., Dinoor, A., Ellwood, S. R., Graf, J., Hatta, K., Helguera, M., Sánchez-Martín, J., McDonald, B. A., Morgounov, A. I., Müller, M. C., Shamanin, V., Shimizu, K. K., Yoshihira, T., Zbinden, H., Keller, B., and Wicker, T. 2022. Global genomic analyses of wheat powdery mildew reveal association of pathogen spread with historical human migration and trade. *Nat. Commun.* 13:4315.
- Syme, R. A., Martin, A., Wyatt, N. A., Lawrence, J. A., Muria-Gonzalez, M. J., Friesen, T. L., and Ellwood, S. R. 2018. Transposable element genomic fissuring in *Pyrenophora teres* is associated with genome expansion and dynamics of host-pathogen genetic interactions. *Front. Genet.* 9:130.
- Turo, C., Mair, W., Martin, A., Ellwood, S., Oliver, R., and Lopez-Ruiz, F. 2021. Species hybridisation and clonal expansion as a new fungicide resistance evolutionary mechanism in *Pyrenophora teres* spp. *bioRxiv* 454422.
- Vasighzadeh, A., Sharifnabi, B., Javan-Nikkhah, M., Seifollahi, E., Landermann-Habetha, D., Feurtey, A., and Holtgrewe-Stukenbrock, E. 2021. Population genetic structure of four regional populations of the

- barley pathogen *Pyrenophora teres* f. *maculata* in Iran is characterized by high genetic diversity and sexual recombination. *Plant Pathol.* 70: 735-744.
- Williams, K. J., Lichon, A., Gianquitto, P., Kretschmer, J. M., Karakousis, A., Manning, S., Langridge, P., and Wallwork, H. 1999. Identification and mapping of a gene conferring resistance to the spot form of net blotch (*Pyrenophora teres* f. *maculata*) in barley. *Theor. Appl. Genet.* 99:323-327.
- Wright, S. I., Lauga, B., and Charlesworth, D. 2003. Subdivision and haplotype structure in natural populations of *Arabidopsis lyrata*. *Mol. Ecol.* 12:1247-1263.
- Yoshida, Y. 1993. Lanosterol 14 $\alpha$ -demethylase (cytochrome P45014DM). Pages 627-639 in: *Cytochrome P450*. J. B. Schenkman and H. Greim, eds. Springer, Berlin, Heidelberg, Germany.
- Yuzon, J. D., Wyatt, N. A., Vasighzadeh, A., Clare, S., Navratil, E., Friesen, T. L., and Stukenbrock, E. H. 2023. Hybrid inferiority and genetic incompatibilities drive divergence of fungal pathogens infecting the same host. *Genetics* 224:iyad037.
- Zohary, D., and Hopf, M. 2000. *Domestication of Plants in the Old World: The Origin and Spread of Cultivated Plants in West Asia, Europe, and the Nile Valley*. Oxford University Press, Oxford, U.K.